The EMBO Journal (2010) 29, 2315–2328 | © 2010 European Molecular Biology Organization | All Rights Reserved 0261-4189/10
www.embojournal.org

THE EMBO JOURNAL

Cooperative interactions at the SLP-76 complex are critical for actin polymerization

Mira Barda-Saad[1,*], Naoto Shirasu[2], Maor H Pauker[1], Nirit Hassan[1], Orly Perl[1], Andrea Balbo[3], Hiroshi Yamaguchi[4], Jon CD Houtman[5], Ettore Appella[4], Peter Schuck[3] and Lawrence E Samelson[2]

[1]Mina and Everard Goodman Faculty of Life Sciences, Bar-Ilan University, Ramat-Gan, Israel, [2]Laboratory of Cellular and Molecular Biology, Center for Cancer Research, NCI, Bethesda, MD, USA, [3]Dynamics of Macromolecular Assembly, Laboratory of Bioengineering and Physical Science, NIBIB, National Institutes of Health, Bethesda, MD, USA, [4]Laboratory of Cell Biology, NCI, Bethesda, MD, USA and [5]Department of Microbiology, University of Iowa, Iowa City, IA, USA

T-cell antigen receptor (TCR) engagement induces formation of multi-protein signalling complexes essential for regulating T-cell functions. Generation of a complex of SLP-76, Nck and VAV1 is crucial for regulation of the actin machinery. We define the composition, stoichiometry and specificity of interactions in the SLP-76, Nck and VAV1 complex. Our data reveal that this complex can contain one SLP-76 molecule, two Nck and two VAV1 molecules. A direct interaction between Nck and VAV1 is mediated by binding between the C-terminal SH3 domain of Nck and the VAV1 N-terminal SH3 domain. Disruption of the VAV1:Nck interaction deleteriously affected actin polymerization. These novel findings shed new light on the mechanism of actin polymerization after T-cell activation.
The EMBO Journal (2010) **29,** 2315–2328. doi:10.1038/emboj.2010.133; Published online 18 June 2010
Subject Categories: signal transduction; immunology
Keywords: actin polymerization; lymphocyte activation; signalling complexes; SLP-76

Introduction

Actin polymerization in T cells is induced after engagement of the T-cell antigen receptor (TCR). In addition to controlling cellular shape and polarity, this process regulates vital T-cell responses, such as T-cell activation, adhesion and proliferation. Alterations in dynamic actin cytoskeletal rearrangement can also result in immunodeficiency. Multiple signalling cascades link the TCR to actin polymerization (Bubeck Wardenburg *et al*, 1998; Bunnell *et al*, 2001; Cannon *et al*, 2001; Badour *et al*, 2003; Barda-Saad *et al*, 2005; Dombroski *et al*, 2005; Nolz *et al*, 2006). Immediately after TCR engagement, several protein tyrosine kinases are activated leading to phosphorylation of TCR components and various effector molecules (Kane *et al*, 2000). One of these effector proteins is the transmembrane adapter, linker for activation of T cells (LAT) (Zhang *et al*, 1998). LAT is rapidly phosphorylated on conserved tyrosines and, once phosphorylated, directly binds to the SH2 domains of several proteins, including Grb2, Grb2-related adaptor protein (Gads) and phospholipase Cγ1 (PLCγ1).

The recruitment of SLP-76 also brings a number of additional associated molecules into LAT-nucleated signalling complexes. SLP-76-binding proteins include, among others, the Rho-family GTPase exchange factor (GEF), VAV1, the Nck adapter molecule and the nucleation-promoting factors (NPFs) including the Wiskott–Aldrich syndrome family protein (WASp), key regulators of the actin cytoskeleton (Wu and Koretzky, 2004; Smith-Garvin *et al*, 2009). Several lines of evidence suggest that phosphorylation of SLP-76 is critical to bring VAV1 and Nck into proximity (Raab *et al*, 1997; Bubeck Wardenburg *et al*, 1998; Zeng *et al*, 2003). VAV1 then activates the small G-proteins including Cdc42 (GTP-Cdc42) and Rac (Rac-GTP) specifically at the site of TCR signalling, whereas Nck recruits NPFs to the same site (Buday *et al*, 2002; Tybulewicz, 2005). NPF activation leads to the activation of the Arp2/3 complex, which induces the nucleation of branched actin filaments at the site of the T-cell/antigen-presenting cell interface, and to the formation of the immunological synapse (IS) (Fuller *et al*, 2003; Billadeau and Burkhardt, 2006; Burkhardt *et al*, 2008; Dustin, 2008).

Structure-function studies of SLP-76 have shown the importance of multiple SLP-76 domains in TCR signalling. SLP-76 consists of at least four domains: (1) the N-terminal sterile α motif (SAM) domain; (2) an acidic domain containing three tyrosine residues subject to phosphorylation: Y113 (in humans, Y112 in mice), Y128 and Y145; (3) the central proline-rich domain that mediates the interactions with Gads and PLCγ1 and (4) the C-terminal SH2 domain that binds to the adhesion- and degranulation-promoting adaptor protein (ADAP) and to the hematopoietic progenitor kinase 1 (HPK1) (Fang *et al*, 1996; Zeng *et al*, 2003; Wu and Koretzky, 2004; Kliche *et al*, 2006; Koretzky *et al*, 2006).

It has been demonstrated that although phosphorylation of Y113 and Y128 enables the binding of SLP-76 to either VAV1 or Nck, the interaction of SLP-76 with Nck is more dependent on phosphorylation of Y128 than Y113 (Wu *et al*, 1996; Bubeck Wardenburg *et al*, 1998; Wunderlich *et al*, 1999; Jordan *et al*, 2006). Y145 is important for optimal association of SLP-76 with the inducible tyrosine kinase, Itk, a key regulator of T-cell function (Wunderlich *et al*, 1999; Bunnell *et al*, 2000; Clements, 2003; Dombroski *et al*, 2005). Recent studies using a panel of murine SLP-76 tyrosine mutants demonstrated that phosphorylation of Y112 and Y128 facilitates the phosphorylation of Y145, suggesting a functional hierarchy among SLP-76 tyrosines (Jordan *et al*, 2006). However, to date, there are no definitive measurements of binding at these phosphorylation sites, and details of protein interactions at this domain of SLP-76 are still lacking.

*Corresponding author. Mina and Everard Goodman Faculty of Life Sciences, Bar-Ilan University, Building 204, Rm. 210, Ramat-Gan 52900, Israel. Tel.: +972 3 5317311; Fax: +972 3 7384058;
E-mail: bardasm@mail.biu.ac.il

Received: 26 December 2009; accepted: 25 May 2010; published online: 18 June 2010

Earlier, we have taken a multi-dimensional approach to the study of the binding interactions of multi-molecular complexes. For example, we used fluorescence resonance energy transfer (FRET) to follow the interactions between Nck and WASp, which leads to actin polymerization (Barda-Saad *et al*, 2005). In other studies, we measured thermodynamic parameters and calculated the binding affinity of LAT to the SH2-containing proteins Grb2, Gads and PLCγ1 using isothermal titration calorimetry (ITC) (Houtman *et al*, 2004, 2006, 2007). Our studies provided a description of the highly cooperative nature of the interactions of Gads, SLP-76 PLCγ1 and LAT during the formation of signalling complexes (Houtman *et al*, 2004, 2006). In one of these earlier studies, we focused on the interactions of SLP-76 at its proline-rich central domain. In the current work, we have turned to the SLP-76 acidic domain, the site of tyrosine phosphorylation and binding of VAV1, Nck and Itk. In this study, we take a multi-disciplinary approach by using molecular imaging, FRET analysis and biophysical techniques to focus on the binding properties of SLP-76, Nck and VAV1 and their multi-molecular interactions. Our data reveal an unexpected stoichiometry of association and an unexpected direct molecular association between Nck and VAV1. We show the functional importance of this direct association and demonstrate the cooperative nature of the multi-molecular interaction, which is critical to the regulation of actin dynamics in activated T cells.

Results

Evaluation of Nck and VAV1 binding to SLP-76 using ITC

Our study began with an analysis of Nck and VAV1 binding to SLP-76. ITC experiments were performed with purified full-length Nck and a large polypeptide fragment of VAV1 to measure their specificity of binding and binding affinities to short or long synthesized SLP-76 phosphopeptides (Supplementary Figure S1A–C; Supplementary Table S1) (Houtman *et al*, 2004, 2006; Ladbury, 2007). As detailed in the Supplementary data, these studies show that at least two molecules of VAV1 or Nck can associate with one molecule of SLP-76. These data also imply that VAV1 and Nck can bind directly.

Analytical ultracentrifugation studies of VAV1 and Nck binding to SLP-76

We turned to analytical ultracentrifugation (AUC) to further pursue these complex-binding events, to confirm higher-order protein complex formation, and to determine whether there is cooperativity of binding at SLP-76 in the presence of VAV1, Nck or both.

We used labelled VAV1-FAM (after verifying by ITC that VAV1-FAM has the same binding constant to SLPpY128 as unlabelled VAV1) (as described in detail in Supplementary data), unlabelled Nck and rhodamine TAMRA end-labelled SLP-76 phosphopeptides. The multi-signal sedimentation coefficient distribution analysis then can display the distribution of *s*-values (Sv) specifically of all species containing SLP-76 ($c_{SLP}(s)$), VAV1 ($c_{VAV}(s)$) and Nck ($c_{Nck}(s)$) coexisting in the same sample.

We conducted preliminary experiments with SLP-76 peptides alone (Figure 1A), with VAV1-FAM alone, and with Nck alone (Figure 1B). The preparation of VAV1-FAM showed some contaminations with irreversible VAV1-FAM oligomers ($\sim$15), which could not be further purified. However, by considering only $c_{SLP}(s)$ from SLP-76-containing species, VAV1:SLP-76 complexes could still be rigorously characterized. With free SLP-76 peptides sedimenting at $\sim$1.2 S, all contributions to $c_{SLP}(s)$ $>$2 S are peptides bound to VAV1 or Nck. We recorded their weight-average *s*-value (s_w) to estimate their average size (Table I). Only for the largest mixed complexes observed in experiments with ternary mixtures (magenta line in Figure 1C) were the *s*-values higher than the contaminants of VAV1 and Nck, so that the sedimentation coefficient $c_{VAV}(s)$ and $c_{Nck}(s)$ allowed us to assess the stoichiometry of VAV1-FAM and Nck in the mixed complexes.

When we studied mixtures of VAV1:SLP-76 and Nck:SLP-76 separately, we observed that the size of the complexes with SLP-76 increased with the triple phosphorylated peptide relative to both double phosphorylated complexes. This is illustrated in Figure 1A for VAV1 where for both doubly phosphorylated SLP-76 peptides the main $c_{SLP}(s)$ peak was found at *s*-values only slightly higher than that of VAV1-FAM ($\sim$3 S, commensurate with the small increase of the complex molar mass compared to the mass of VAV1-FAM alone). However, for pY113,128,145 $c_{SLP}(s)$ exhibited a strong peak at 4.2 S. It is not possible to directly conclude from the *s*-value what the molar mass of this species is due to uncertainties of hydrodynamic shape and because the reaction boundary of a rapidly interacting system always sediments slower than the sedimentation coefficient of the complex species. Assuming no drastic change in the translational friction coefficient between the ligated and unligated protein, we could estimate lower limits of the complex molar mass. For the VAV1—SLPpY113, 128, 145 being $\sim$4.2 S, the complex is likely $>$60 kDa, that is containing two VAV1 molecules. It is highly unlikely that this peak represents binding to VAV1 dimer fraction, as a much lower amount of the 4.2 S populations were observed with the double phosphorylated SLP-76 peptides despite their higher affinity for VAV1 (Supplementary Table S1). This result corroborates the finding by ITC that the triple phosphorylated peptide offers two binding sites. Similar results were found for Nck binding to SLP-76 peptides (Table I). As in the analogous experiments with VAV1, a significant shift of the peak *s*-value is observed, again supporting the observation by ITC of two simultaneous Nck sites on the triple phosphorylated peptide.

Next we asked whether offering both VAV1 and Nck to the SLP-76 peptides could lead to mixed triple complexes. In a control experiment with VAV1-FAM and Nck at 4 μM in the absence of SLP-76, we only observed a slight increase ($\sim$0.15 S) of the sedimentation coefficients of the mixture over the individual free components, indicating weak and rapidly reversible binding of the purified molecules in solution (data not shown). Figure 1B shows the sedimentation coefficient distribution $c_{SLP}(s)$ of SLPpY113, 145 containing species in the presence of VAV1, Nck, and both VAV1 and Nck. A slightly higher average sedimentation rate of the complexes is observed for the binary mixture with SLP-76:Nck relative to SLP-76:VAV1, likely because of the higher molar mass of Nck ($\sim$47 versus $\sim$32 kDa for VAV1). However, a drastic shift was observed in the simultaneous presence of both VAV1 and Nck under otherwise identical conditions (magenta line, compared with blue and green lines for the individual proteins), clearly demonstrating the

formation of mixed complexes on a peptide previously shown to bind only one protein.

The *s*-value of the main peak of the ternary mixture is consistent with that of a 1:1:1 complex, and the absence of the ~3–3.5 S species predominant for the binary mixtures suggests the possibility of cooperative binding of VAV1 and Nck to SLP-76. Unfortunately, these data do not allow us to distinguish possible structural configurations and answer whether both proteins bound by each making contact to different sites on SLP-76, or VAV1 bound to Nck on a preformed Nck:SLP-76 complex.

We have seen that, on one hand, phosphorylation at all three tyrosines 113, 128 and 145 allows for two binding sites each for VAV1 and Nck, and on the other hand, that VAV1 and Nck can bind simultaneously, possibly cooperatively, to the same double phosphorylated SLP-76 peptide. Thus, we asked whether the presence of both proteins in solution with the triple phosphorylated peptide could generate even larger complexes. We conducted sedimentation experiments with the SLPpY113, 128, 145 peptide with VAV1, Nck and VAV1 + Nck (Figure 1C). Strikingly, a large shift in the peak *s*-value of the $c_{SLP}(s)$ distribution of the ternary mixture can be discerned relative to either VAV1:SLP-76 or Nck:SLP-76, as well as the absence of species with sedimentation coefficients of ~4 S that were predominant in the binary mixtures. This indicates the cooperative formation of larger mixed multi-protein complexes. The weighted-average s_w value of 5.6 S corresponds (assuming a translational frictional coefficient similar to the free proteins) to molar masses >107 kDa, suggesting the presence of a complex with at least three, or possibly four proteins per SLP-76 peptide. Interestingly, the relative peak areas of the different distributions suggest a 2:2:1 VAV1:Nck:SLP-76 molar ratio (on average) for the 6 S species. The data are not consistent with a complex comprised of multiple SLP-76 molecules associated with Nck and VAV1 at the measured ratio. For example, a dimer of SLP-76 with Nck and VAV1 (with a ratio of 4:4:2) would have an apparent molecular weight of 350 kDa and would migrate at

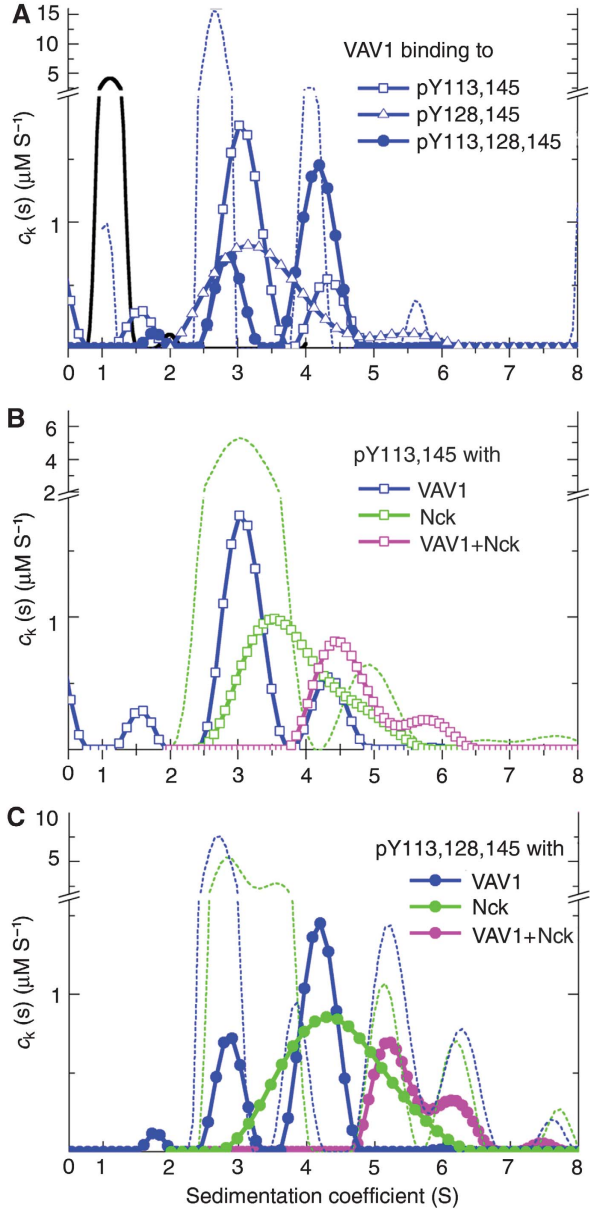

Table I Complex formation of VAV and Nck with phosphorylated 49mer SLP-76 peptides by sedimentation velocity

Interaction	Weighted-average s_w-value of complexes (S)[a]	Concentration of SLP-76 in complexes (μM)
VAV–SLPpY113,145	3.4	1.5
VAV–SLPpY128,145	3.4	1.5
VAV–SLPpY113,128,145	3.8	1.2
Nck–SLPpY113,145	3.8	1.5
Nck–SLPpY128,145	3.9	1.3
Nck–SLPpY113,128,145	4.4	1.6
VAV–Nck–SLPpY113,145	4.8	1.0
VAV–Nck–SLPpY128,145	4.8	1.0
VAV–Nck–SLPpY113,128,145	5.6	0.7

[a]Calculated by integration of $c_{SLP}(s)$ over all populations >2 S.

Figure 1 SLP-76, Nck and VAV1 complex formation. Sedimentation coefficient distributions $c_k(s)$ of the SLP-76 complexes formed in the presence of Nck and/or VAV1. The data are from sedimentation velocity experiments with different mixtures, of SLP-76 peptides pY113pY145 (squares), pY128pY145 (triangles) or pY113pY128pY145 (circles), all at 1.5 μM, in the presence of 6 μM VAV1 (blue), 6 μM Nck (green) or both (magenta). All data shown with symbols and/or solid lines are $c_{SLP}(s)$ distributions of SLP-76 peptides and its complexes only, calculated by exploiting a spectrally distinct chromophoric label. In the presence of protein, the peptides track the sedimentation of complexes at *s*-values >2 S. (**A**) The control sedimentation coefficient distribution of SLP-76 peptides alone is shown as black solid line. The result of a control experiment with VAV1 alone is shown as blue dotted line, which displays $c_{VAV}(s)$ calculated by taking advantage of its own characteristic spectral properties of the FAM label on VAV1. In the presence of the triply phosphorylated peptide, a population of 4.2 S complexes (likely in 2:1 stoichiometry) can be discerned. (**B**) VAV1 and Nck can both simultaneously bind to SLP-76 pY113,145, as can be discerned from the shift towards faster-sedimenting complexes in the presence of VAV1 + Nck. The sedimentation coefficient distribution from an experiment with Nck alone, as observed through its own specific spectral signature $c_{Nck}(s)$, is shown as dotted line. (**C**) Higher-order complexes are formed on the triply phosphorylated peptide in the presence of VAV1 + Nck. For the experiment with both proteins (magenta), the dotted lines show the sedimentation coefficient distributions calculated from multi-signal analysis for VAV1-containing complexes $c_{VAV}(s)$ (blue dotted line) and Nck-containing complexes $c_{Nck}(s)$ (green dotted line) in the same solution.

>10 S. Thus, our data unequivocally show the formation of a mixed multi-protein complex on a multiply phosphorylated SLP-76 peptide *in vitro*.

The formation of the Nck, VAV1 and SLP-76 triple molecular complex

The preceding analysis of VAV1, Nck and SLP-76 resulted in the determination of basic binding parameters and the conclusion that these proteins can interact to create a multi-molecular complex at the N-terminal region of SLP-76. To independently confirm a multi-molecular complex simultaneously containing VAV1, Nck and SLP-76, and to examine such complexes *in vivo*, we used a molecular imaging approach (Barda-Saad *et al*, 2005; Houtman *et al*, 2006). T cells expressing fluorescently tagged versions of Nck or VAV1 were dropped onto a surface coated with a stimulatory monoclonal antibody that binds the TCR. Activation resulted in recruitment of multiple signalling molecules, including the tagged versions, to cluster at the points of contact with the stimulatory surface. These structures are known as signalling microclusters. This process leads to activation of tyrosine kinases, intracellular calcium elevation and cellular spreading, all functions seen with normal T-cell activation.

To assess the possibility of a trimolecular complex containing VAV1, Nck and SLP-76 by imaging, we studied the binding of these proteins by a pairwise analysis of colocalization and, more definitively, FRET (Barda-Saad *et al*, 2005; Wallrabe and Periasamy, 2005; Sohn *et al*, 2006). We determined FRET between yellow fluorescent protein (YFP) and cyan fluorescent protein (CFP) tagged to either VAV1, Nck or SLP-76. The association of wild-type (wt) versions of these proteins in stimulated T-cell lines was examined by using mutant T cells (J14 and J-VAV) lacking the expression of specific signalling proteins (SLP-76 and VAV1, respectively) versus their reconstituted counterparts (Yablonski *et al*, 1998; Cao *et al*, 2002). Where mutant T cells were not available, as in the case of Nck, gene-targeting approaches to silence both Nckα and Nckβ using small interfering RNA (siRNA) were used.

VAV proteins are not required for the association of Nck to SLP-76

Nck recruitment to signalling clusters has been observed earlier (Zeng *et al*, 2003; Barda-Saad *et al*, 2005). To determine whether Nck can bind to SLP-76 independently of VAV proteins, we used the mutant Jurkat T cell, J-VAV, which lacks the expression of VAV1 protein. Both CFP-SLP-76 and YFP-Nck were then expressed in these cells (Figure 2A). FRET analysis in live activated T cells showed that Nck associated with SLP-76 and was recruited to the TCR signalling complex in the absence of VAV1. No differences in the FRET efficiency was measured in J-VAV cells lacking VAV1 (22.7% ± 2) compared with J14 cells reconstituted with YFP-SLP-76 (27.5% ± 5.5) ($P \leqslant 0.094$). To eliminate the possibility that VAV2 and VAV3 isoforms expressed in J-VAV cells recruit Nck to SLP-76, gene silencing of these isoforms was performed and FRET efficiency between SLP-76 to Nck was measured (Supplementary Figure S2A). Our results indicate that VAV proteins were not required for the stabilization of the molecular interaction between Nck and SLP-76 (Figure 2A; Supplementary Figure S2A). These results are consistent with the earlier biophysical binding data.

Nck is required for the recruitment of VAV1 to SLP-76

To test whether VAV1 binds SLP-76 without Nck, we used J14 SLP-76-deficient T cells expressing YFP-SLP-76 and VAV1-CFP. Gene silencing was used to regulate Nck expression. We used siRNA specific for the SH2 domains of Nck α and β (Figure 2B). Treatment of YFP-SLP-76 VAV1-CFP, J14 with Nck-specific siRNA resulted in ∼90% reduction in Nck expression in comparison to almost no effect with irrelevant siRNA (Figure 2B). When control siRNA oligos were used (Figure 2C), FRET levels between SLP-76 and VAV1 were readily detected (18.9% ± 1.5). However, FRET efficiency between SLP-76 and VAV1 was dramatically reduced ($P \leqslant 0.000015$) between these two proteins in Nck gene silenced cells (3% ± 2). These results indicate that optimal VAV1 binding to SLP-76 in activated Jurkat T cells requires the presence of Nck.

The FRET data thus indicate that VAV1 binding to SLP-76 *in vivo* is dependent on the Nck–SLP-76 interaction. These results in combination with our biophysical data, suggesting a VAV1:Nck:SLP-76 binding stoichiometry of 2:2:1 lead to two important predictions. First, disruption of each of the two specific sites of interaction between Nck and SLP-76 should partially block VAV1 interaction with SLP-76, whereas disruption of both sites would be more dramatic. Second, VAV1 and Nck must directly interact. To test the first prediction, VAV1-deficient J-VAV cells expressing VAV1-YFP were transiently transfected with constructs expressing SLP-76 mutated at tyrosine 113 (Y113F) or tyrosine 128 (Y128F) or at both sites (Y113, 128F). FRET analysis was performed to follow the interaction between VAV1 and SLP-76 mutants compared with VAV1 and SLP-76 wt. Our data indicate that point mutation at each site (Y113F or Y128F) individually partially reduced the FRET efficiency between VAV1 and SLP-76, whereas a double mutation (Y113, 128F) dramatically abolished this interaction (Supplementary Figure S2B). Assuming that Nck binding to SLP-76 is required for VAV1–SLP-76 interactions (Figure 2C), this result shows that each Nck-binding site recruits a VAV1 molecule. This experiment thus also provides strong support for the biophysical results. Each of the two Nck sites supports binding to a VAV1 molecule and therefore two VAV1 molecules and two Nck molecules can bind SLP-76.

SLP-76 is not required for the molecular association between Nck and VAV1

Our second prediction, that Nck binds VAV1 directly in cells, was tested next. We used the T-cell spreading assay, to determine the distribution of Nck and VAV1 in the presence or absence of SLP-76. Nck-YFP and VAV1-CFP interactions were examined in wt Jurkat E6.1 cells, SLP-76-deficient J14 cells or in J14 cells reconstituted with wt SLP-76 (SLP-76 wt, J14). Our results showed that stimulation of E6.1 cells stably expressing VAV1 and Nck resulted in the formation of signalling clusters containing both molecules (Figure 3A). In the absence of SLP-76 (J14 cells), the distribution of Nck and VAV1 was altered. The proteins remained homogenously dispersed in the cytosol and no clusters were observed. These data are consistent with our earlier findings (Barda-Saad *et al*, 2005; Braiman *et al*, 2006), indicating altered Nck and VAV1 recruitment to the TCR sites in the absence of SLP-76. Surprisingly, no significant alterations ($P \leqslant 0.07$) in the FRET efficiency was measured between Nck and VAV1 in the

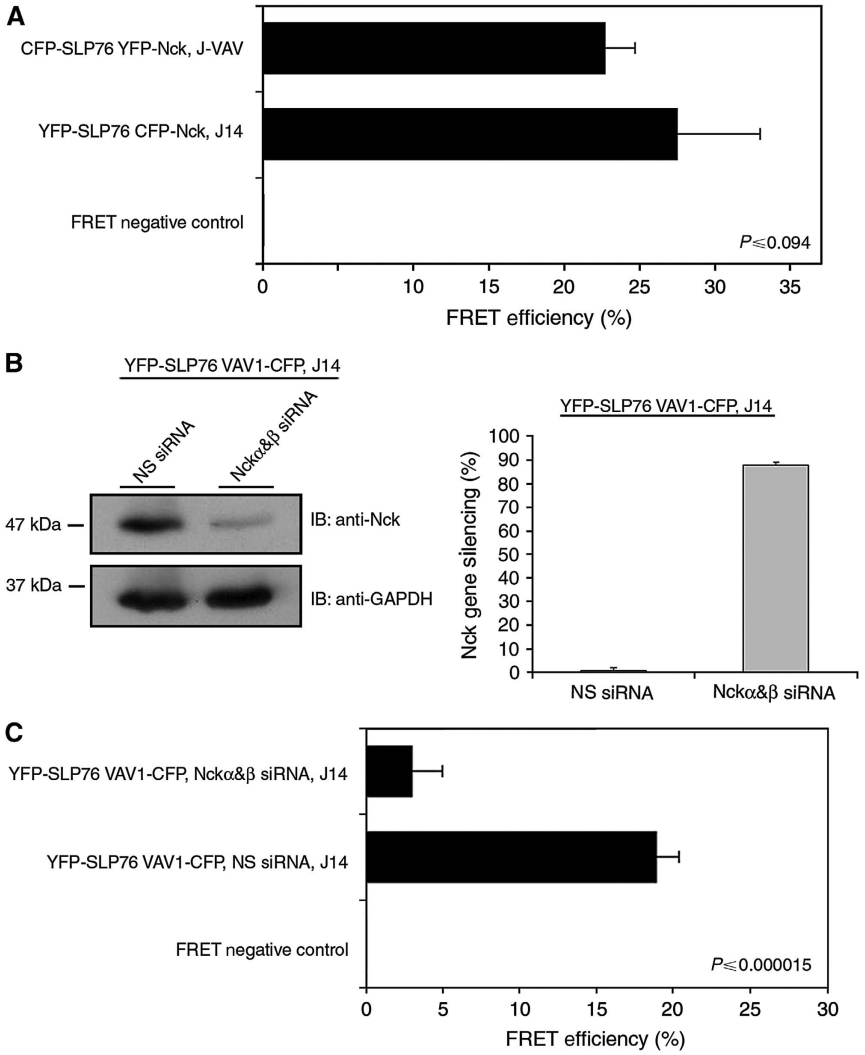

Figure 2 FRET analysis of the triple molecular complex SLP-76, Nck and VAV1. (**A**) SLP-76-deficient Jurkat J14 cells were reconstituted with YFP-SLP-76 and transfected with CFP-Nck. VAV1-deficient Jurkat J-VAV cells were cotransfected with CFP-SLP-76 and YFP-Nck. High FRET efficiency was observed in the presence, as well as in the absence, of VAV1 ($P \leqslant 0.094$). (**B**) J14 cells expressing YFP-SLP-76 CFP-Nck were transiently transfected with double-stranded siRNA oligonucleotides comprising Nckα&β SH2 domain-specific sequences or a non-specific sequence (negative control). At 48 h after transfection, cells were analysed as described above for protein levels of Nck using anti-Nck antibody. The siRNA-mediated Nck downregulation was compared with the level of GAPDH. (**C**) J14 cells were reconstituted with YFP-SLP-76 and transfected with VAV1-CFP. The decrease in FRET efficiency using Nckα&β siRNA shows that Nck is essential for the recruitment of VAV1 to SLP-76 signalling complexes ($P \leqslant 0.000015$). The results are based on more than three independent experiments.

presence (25.9% ± 1) or the absence (22.6% ± 1.2) of SLP-76 (J14) (Figure 3A). J14 cells reconstituted with SLP-76 demonstrated FRET efficiency of about 25.6% ± 7.5 between Nck to VAV1 similar to that observed in E6.1 (Figure 3A). As FRET can occur between fluorescent species separated no further than ~10 nm, detection of FRET between these two molecules strongly suggests their direct interaction.

To confirm a direct VAV1–Nck interaction, we subjected cell lysates from E6.1, SLP-76-deficient or VAV1-deficient T cells to immunoprecipitation with anti-Nck antibody and blotting with anti-VAV1 antibody (Figure 3B; Supplementary Figure S2C and S2D). As a control for the specificity of the immunoprecipitation, we used cell lysates of VAV1-deficient T cells. No non-specific binding was observed between Nck to the anti-VAV1 beads (Figure S2C). The protein level of VAV1 (the 122 kDa chimeric protein) was determined and found to be 1.4-fold higher in J14 than the overexpressed protein in E6.1 cells, however, similar (1.05-fold) to endogenous VAV1 (Supplementary Figure S2D). In agreement with the imaging results, Nck coprecipitated with VAV1 both in stimulated and non-stimulated wt, Jurkat E6.1 cells and in SLP-76-deficient T cells, J14 (Figure 3B), indicating a constitutive interaction between the two proteins independent of SLP-76.

To demonstrate that the interaction between Nck and VAV1 occurs independently of the acidic domain of SLP-76, we transiently expressed SLP-76 wt or SLP-76 mutated at tyrosines 113, 128 and 145 (Y3F) in SLP-76-deficient T cells, J14 cells. Cell lysates were prepared and immunoprecipitated with anti-VAV1 and blotted with anti-Nck. Our data clearly indicate a constitutive interaction between VAV1 and Nck regardless of whether wt or Y3F SLP-76 is expressed. The association of Nck and VAV1 seemed to be increased in stimulated SLP-76 wt compared with J14 cells though the difference was not significantly different (Figure 3C).

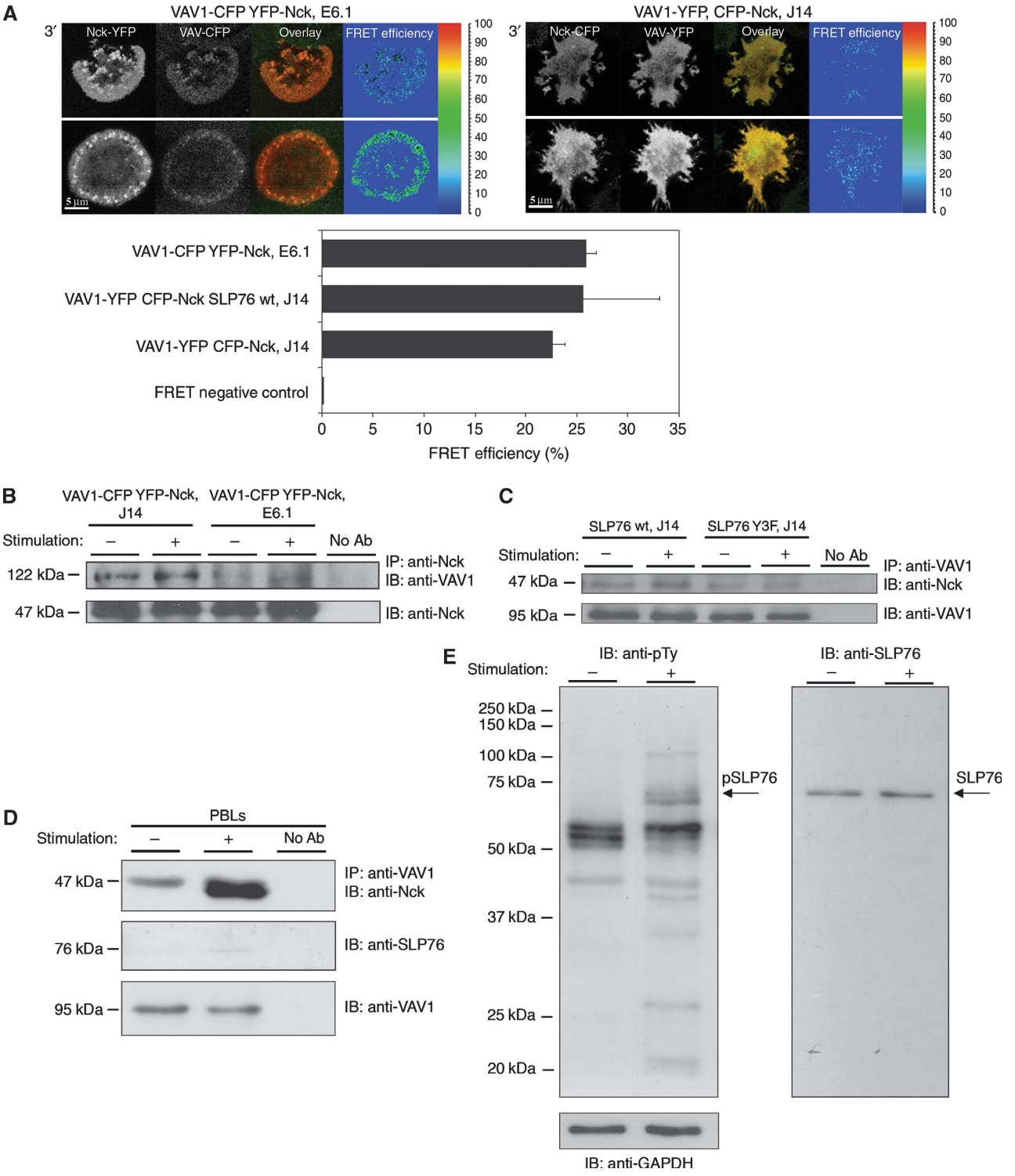

Figure 3 The interaction between Nck and VAV1 is independent of SLP-76. (**A**) FRET analysis of the molecular interaction between Nck and VAV1 in Jurkat E6.1 T cells expressing YFP-Nck VAV1-CFP was performed in comparison to SLP-76-deficient Jurkat J14 cells ($P \leqslant 0.07$) or J14 reconstituted with SLP-76 wt ($P \leqslant 0.57$) expressing VAV1-YFP CFP-Nck. No significant difference in the FRET efficiency was measured between Nck and VAV1 expressed in J14 to J14 reconstituted with wtSLP-76 cells ($P \leqslant 0.412$). Different cell panels are presented. The results are based on more than five independent experiments. (**B**) Immunoprecipitation assay of the interaction between Nck and VAV1 in the presence of SLP-76, E6.1 Jurkat cells, and in the absence of SLP-76, J14 Jurkat cells. Three independent experiments were performed. One representative experiment is shown. (**C**) J14 cells were reconstituted with SLP-76 wt or SLP-76Y3F mutant form. Immunoprecipitation was performed with anti-VAV1, and the membrane was immunoblotted with anti-VAV1 and anti-Nck. (**D**) Nck and VAV1 interaction was confirmed in PBLs. The molecular interaction was detected in unstimulated as well as TCR-stimulated cells. Six independent experiments were performed. One representative experiment is shown. (**E**) Samples from stimulated and unstimulated PBLs were analysed by western blotting for pSLP-76 levels using anti-phosphotyrosine antibody.

To confirm this finding in normal non-transformed T cells, coprecipitation of VAV1 with Nck was performed in human peripheral blood lymphocytes (PBLs). PBLs were activated as described earlier (Astoul *et al*, 2003; Laurence *et al*, 2004; Barda-Saad *et al*, 2005) with anti-CD3 and anti-CD28. T-cell lysates from unstimulated and stimulated cells were immunoprecipitated with the VAV1 antibody and probed with anti-Nck. Nck proteins could be detected in unstimulated cells, confirming that Nck and VAV1 form a constitutive interaction (Figure 3D). However, the relative amount of the complex was higher in stimulated T cells than that in unstimulated cells, suggesting that this complex is enhanced on T-cell stimulation and phosphorylation of SLP-76 in PBLs as described earlier (Zeng *et al*, 2003). The lysates were thus also probed with anti-phosphotyrosine antibody both to confirm phosphorylation of SLP-76 in the activated cells and to demonstrate the absence of basal phosphorylation of SLP-76 in unstimulated cells (Figure 3E). The results clearly show a constitutive association between Nck and VAV1 in unstimulated primary human T cells, which is further induced on activation. Although a direct interaction between Nck and VAV1 was documented by FRET analysis, we also subjected purified, recombinant Nck and the binding domains of VAV1 (SH3–SH2–SH3) to a direct binding analysis. As noted earlier, a weak binding was seen by AUC, and as well by ITC analyses (data not shown).

The C-terminal SH3 domain of Nck is required for its association with VAV1

We next sought to identify the sites mediating the interaction between Nck and VAV1. Earlier, it was shown that VAV1 binds to the Grb2 C-terminal SH3 domain through its own SH3 domain located on the N-terminal side of the SH2 domain (Ye and Baltimore, 1994; Nishida *et al*, 2001). As a high homology exists between the C-terminal SH3 domain of Grb-2 and SH3 domains of Nck (Supplementary Figure S3), we aimed to assess whether a similar interaction occurs between Nck and VAV1.

To identify which of the three SH3 domains of Nck might mediate the association with VAV1, the three individually SH3-point mutated full-length Nck molecules were checked: the N-terminal SH3 domain (Nck W38K or YFP-Nck*SH3(N)), the central SH3 domain (Nck W143K or YFP-Nck*SH3(mid)) and the C-terminal SH3 adjacent to the SH2 (Nck W229K or YFP-Nck*SH3(C)). The proteins were fluorescently tagged with YFP, and their association to VAV1-CFP was measured in J14, SLP-76-deficient T cells by FRET analysis. Levels of YFP-Nck wt or mutants and VAV1-CFP were appropriate for FRET analysis as detected by FACS analysis (Supplementary Figure S4A and S4B, respectively) and by western blot (Supplementary Figure S4C). FRET efficiency between VAV1-CFP and YFP-Nck wt during T-cell spreading averaged about 32.9% ± 2.3. Our results clearly show a significant reduction in the FRET efficiency between VAV1-CFP and the Nck W229K mutant throughout the spreading process (average of about 9.4% ± 2.4) (Figure 4A). However, no significant differences were measured between VAV1-CFP and the two other constructs, Nck W38K and Nck W143K (Figure 4A and B; Supplementary Figure S4C).

To further examine the association between the C-terminal SH3 domain of Nck with VAV1 and its independence on TCR activation, cell lysates were produced from non-activated and activated stable cells and coimmunoprecipitation between VAV1 and YFP-Nck*SH3(C) or YFP-Nck wt was performed. Levels of YFP-Nck wt and YFP-Nck*SH3(C) were appropriate for immunoprecipitation as detected by FACS analysis and western blot (Supplementary Figure S4D and S4E, respectively). Biochemical analysis (Figure 4C) confirmed the imaging approach. Coimmunoprecipitation between Nck and VAV1 was abolished in the presence of the mutated C-terminal SH3 domain of Nck. Also, the constitutive binding between the two wt proteins was verified.

VAV1 N-terminal SH3 domain is required for the direct interaction with Nck

To determine the site on VAV1 responsible for the interaction with Nck, we again turned to the comparison with VAV1-Grb2 binding. The interaction between VAV1 and Grb2 was shown to involve the proline-rich region located in the N-terminal SH3 domain of VAV1 (Nishida *et al*, 2001). Therefore, we examined whether a mutation in the proline-rich region of the N-terminal SH3 of VAV1 perturbs its binding to Nck. We used a mutant form of VAV1 and determined its association to Nck wt using biochemical coprecipitation and *in vivo* cellular FRET analysis. To examine Nck and VAV1 signalling complex formation in the absence of SLP-76, VAV1-YFP mutated at the proline-rich site, VAV1 W637A was introduced into SLP-76-deficient T cells (J14). No FRET efficiency was measured between VAV1 W637A-YFP and CFP-Nck. In contrast, an average FRET efficiency of about 38.6% ± 3.4 was observed between VAV1 wt-YFP and CFP-Nck (Figure 5A). To verify that the mutation at the VAV1 W637A disrupts Nck–VAV1 association, VAV1 W637A and VAV1 wt were introduced into J-VAV lacking the endogenous form of VAV1 (Figure 5B and C). Although the expression levels of VAV1 W637A-YFP were found higher than the wt both by western blot and FACS analysis (Figure 5B and Supplementary Figure S4F, respectively) coprecipitation of VAV1 and Nck was dramatically reduced in the VAV1 W637A mutant cell lysate in contrast to a constitutive interaction detected between VAV1 wt and endogenous Nck (Figure 5C). In combination, the data shown in Figures 4 and 5 indicate that point mutations in either the C-terminal Nck SH3 domain or the previously known SH3-binding site in VAV1 disrupt the Nck–VAV1 interaction.

The stoichiometric analysis with purified proteins *in vitro* (Figure 1A–C; Supplementary Figure S1A–C) suggests that a 2:2:1 VAV1:Nck:SLP-76 complex can be detected. Such a result can be explained only if there is a direct interaction between Nck and VAV1. To confirm the above *in vivo* findings and better integrate them with the model derived from our biophysical data, VAV1 wt or VAV1 W637A were expressed in VAV1-deficient, J-VAV cells. Cell lysates were prepared and immunoprecipitated with anti-SLP-76 and blotted with anti-VAV1 or anti-Nck (Figure 5D). Our data clearly indicate an interaction between VAV1 wt and SLP-76 in stimulated cells; however, this interaction is substantially reduced in J-VAV cells expressing the VAV1 W637A mutant protein in which the Nck-binding site was abolished. The binding of Nck to SLP-76 is similar in both cell types. These data confirm that the binding of VAV1 to SLP-76 is mainly mediated through the interaction of VAV1 to the Nck bound to SLP-76.

Next, we explored whether Nck–VAV1 interaction is physiologically relevant. As VAV1 has been found to have a

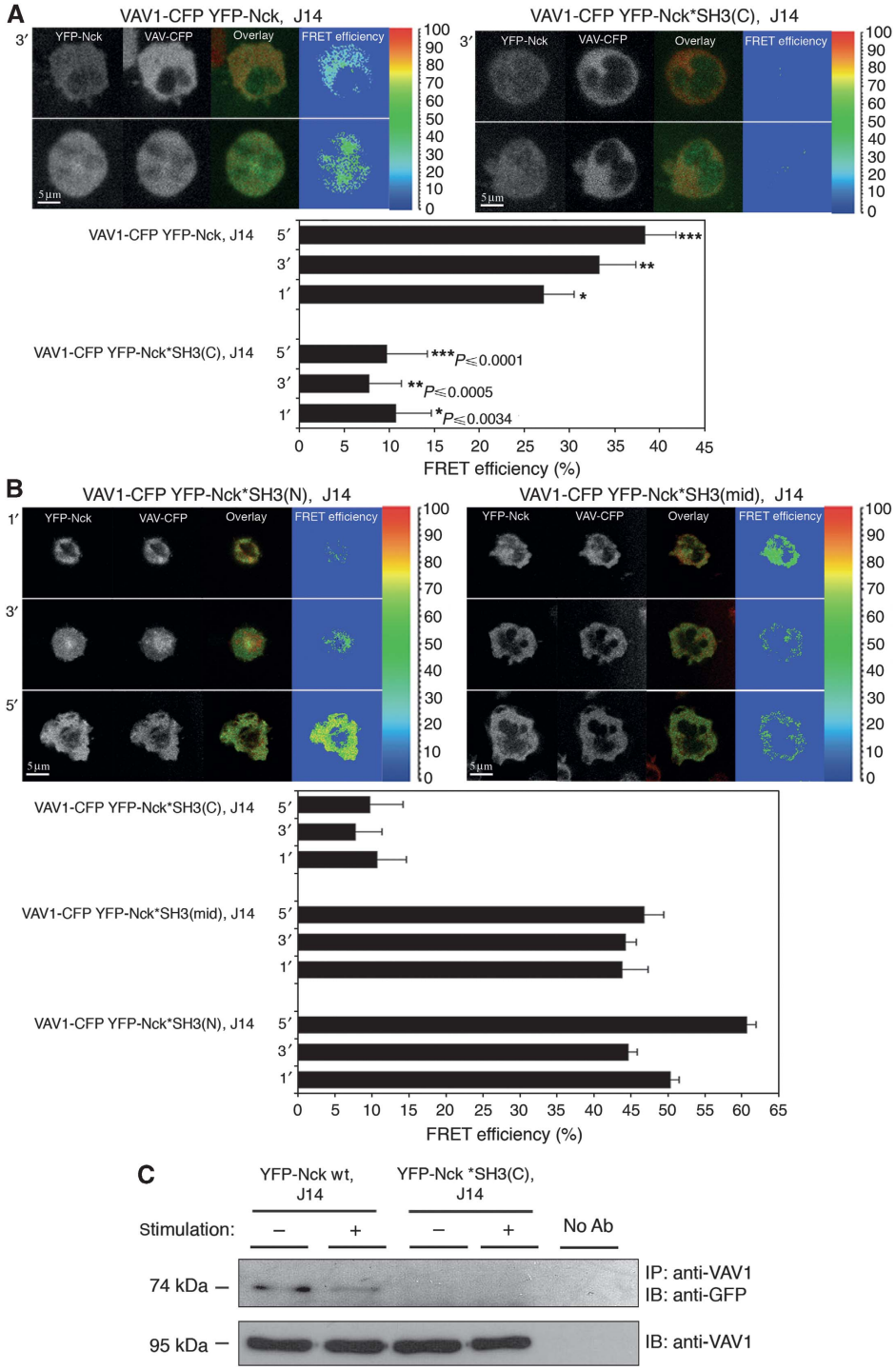

Figure 4 Direct interaction between VAV1 and Nck is mediated by the C-terminal SH3 domain of Nck. (**A**) FRET analysis of the association of Nck wt with VAV1 was determined in J14 cells expressing VAV1-CFP YFP-Nck versus J14 cells expressing Nck mutated at the C-terminal SH3 domain. Different cell panels are presented. (**B**) Mutations at the N- or middle-SH3 domain of Nck were examined as well and compared with the Nck wt. The cells were plated on stimulatory coverslip and fixed after 1, 3 or 5 min. Three independent experiments were performed. (**C**) Immunoprecipitation assay of the interaction between VAV1 wt and Nck wt in comparison to VAV1 wt and mutant form of Nck mutated at C-terminal SH3 domain, Nck*SH3(C) expressed in J14. More than three independent experiments were performed. One representative experiment is shown.

critical function in the regulation of actin polymerization, we explored if a point mutation in the VAV1-binding site for Nck impairs actin polymerization. For this study, actin polymerization was detected by phalloidin staining in VAV1-deficient T cells, J-VAV, and J-VAV cells reconstituted either with VAV1 wt or with VAV1 W637A. Cells reconstituted with VAV1 wt showed a prominent actin ring, similar to normal T cells. Predictably, J-VAV cells exhibited very poor spreading and actin polymerization as quantified by fluorescence intensity (41.88 ± 3.4) (Figure 6A). Strikingly, a similar result was

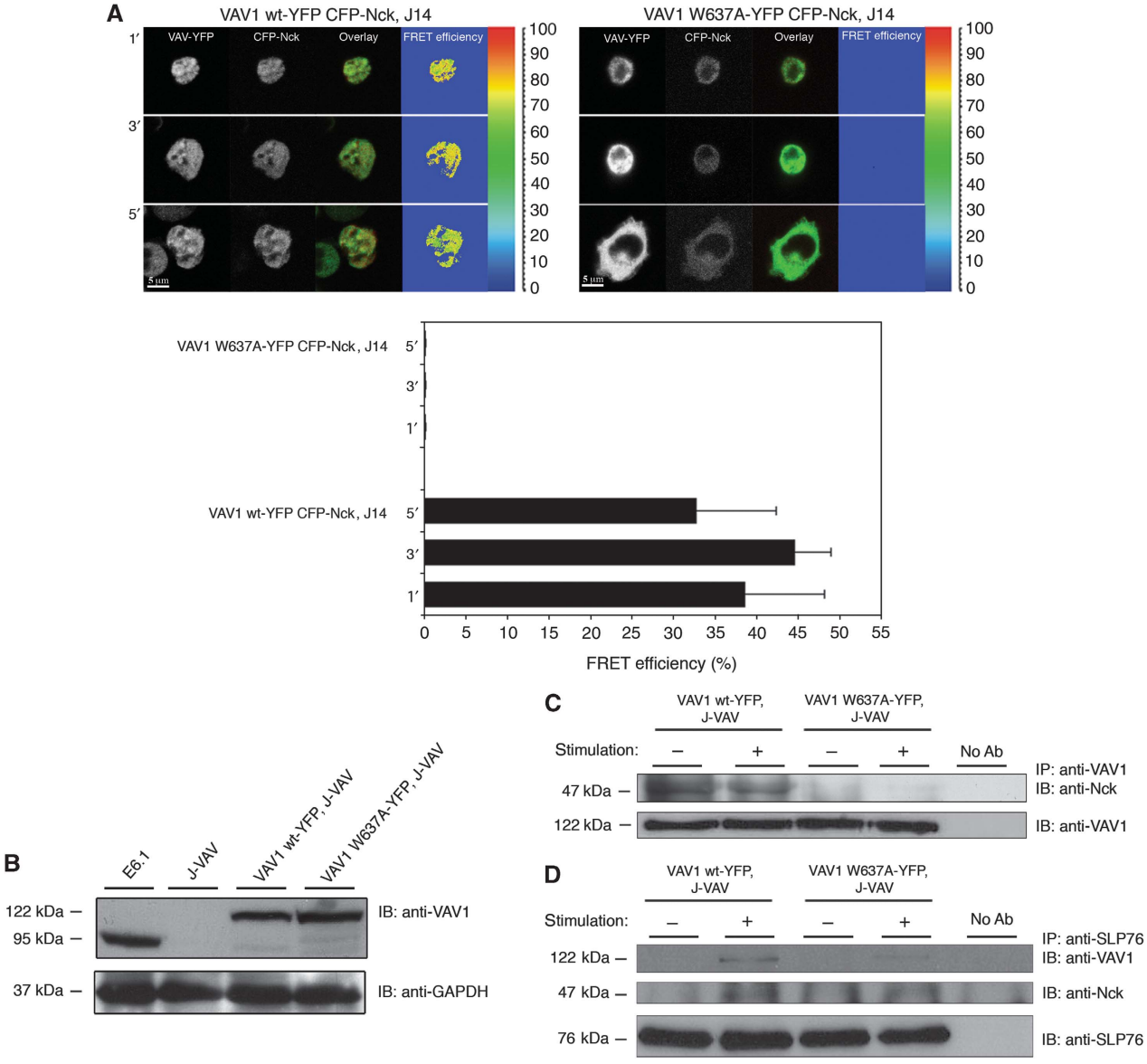

Figure 5 The N-terminal SH3 domain of VAV1 is required for a direct association with Nck. (**A**) FRET analysis of the association of VAV1 with Nck in J14 cells was performed and compared between VAV1 wt-YFP and VAV1 W637A-YFP. The results are based on three independent experiments. (**B**) Analysis of VAV1-deficient cells, J-VAV, stably expressing VAV1 wt-YFP or VAV1 W637A-YFP for their VAV1 protein expression was performed. Cells were lysed. The whole-cell lysates were resolved on SDS–PAGE and probed with anti-VAV1 antibodies to determine protein level expression. (**C**) Immunoprecipitation experiments were performed to detect the interaction between Nck to VAV1 wt or mutated VAV1 W637A form in J-VAV cells. Six independent experiments were performed. One representative experiment is shown. (**D**) The interaction between SLP-76 to VAV1 was detected by immunoprecipitation using VAV1 wt-YFP versus VAV W637A-YFP expressed in J-VAV cells. Immunoprecipitation of SLP-76 and immunoblotting with anti-VAV1 and anti-Nck antibodies were performed.

detected with the VAV1 W637A reconstituted J-VAV cells (59.3 ± 2.2), which showed a significant difference from the J-VAV cells expressing the VAV1 wt form (150.38 ± 6.78) ($P \leqslant 0.00001$). This difference was proven to be not because of low transfection efficiency of the VAV1 forms or poor TCR expression (Figure 5B; Supplementary Figure S4F and data not shown). To eliminate the possibility that the point mutation of VAV1 at the Nck-binding site altered TCR-induced phosphorylation of signalling molecules such as PLCγ1 as determined in J-VAV (Cao *et al*, 2002), the phosphotyrosine profile of VAV1 W637A reconstituted J-VAV cell lysate was compared with J-VAV reconstituted with VAV1 wt and was found to be qualitatively similar (data not shown). These results were supported by the ability of J-VAV stably transfected with wt VAV1 or the mutant VAV1 W637A to flux Ca^{2+} and restore NFAT(IL2)-dependent luciferase expression in response to OKT3 stimulation (data not shown and Figure 6B). Calcium flux of J-VAV reconstituted with VAV1 wt was similar to VAV1 W637A and dramatically different from that in J-VAV as published earlier (Reynolds *et al*, 2002) (data not shown). Interestingly, expression of VAV1 W637A also retained a significant ability to maintain TCR-induced NFAT(IL2) activation similar to VAV1 wt ($P \leqslant 0.59$). These results suggest that although the VAV1 W637A mutant enables signal(s) for NFAT(IL2) activation (Figure 6B), it delivers an impaired signal for actin polymerization.

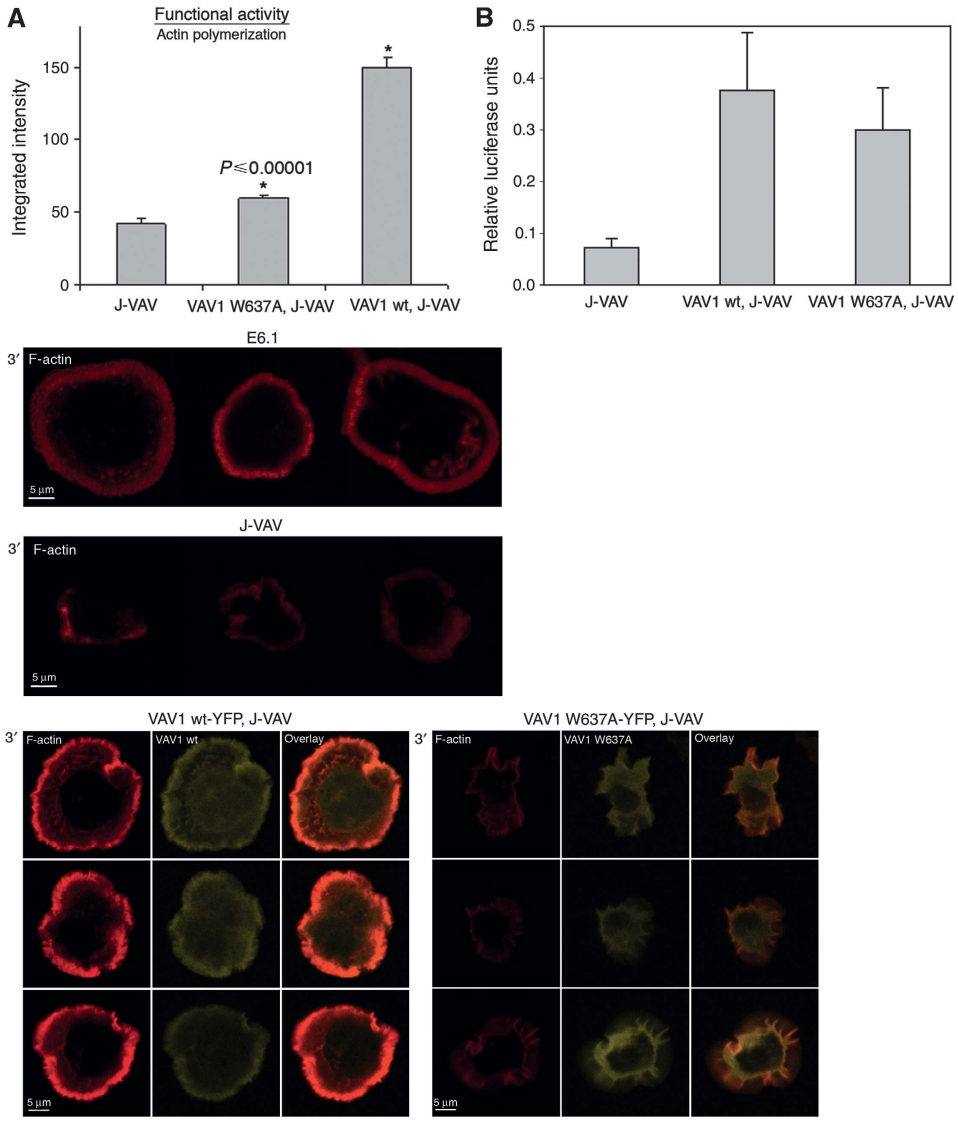

Figure 6 The N-terminal SH3 domain of VAV1 is necessary for an efficient actin polymerization. (**A**) J-VAV cells were reconstituted with VAV1 W637A mutant or VAV1 wt. Cells were seeded over a stimulatory coverslip pre-coated with anti-CD3 antibody then fixed 5 min into the spreading process and their actin polymerization measured by phalloidin staining. The integration of fluorescence intensity of cells labelled with phalloidin is presented. The results were compared with J-VAV cells. Different cell panels are presented. Three independent experiments were performed. (**B**) J-VAV cell lines stably expressing VAV1 wt or VAV1 W637A mutant or vector were transiently cotransfected with an NFAT luciferase reporter plasmid. After 16 h, the cells were incubated for 6 h in tissue culture medium alone (unstimulated), with plate-bound monoclonal antibody to CD3, or with a combination of phorbol 12-myristate 13-acetate (PMA) and ionomycin. Cells were then lysed and assayed for luciferase activity as described in Materials and methods. All values were normalized to internal Renilla controls. The results are expressed as a fraction of the activity obtained on stimulation with PMA and ionomycin. No significant difference was found between VAV1 wt and VAV1 W637A mutant cells ($P \leqslant 0.59$). The results are the average of five independent experiments.

Discussion

Key features of T-cell activation after TCR engagement are the activation of protein tyrosine kinases, the phosphorylation of LAT on multiple tyrosine residues and the recruitment to LAT of additional adapter molecules and enzymes. The multi-domain adapter SLP-76 is central to this process. Many studies have focused on the binding properties of the SLP-76 proline-rich region, which binds Gads and PLCγ1 and the C-terminal SH2 domain, which binds ADAP and HPK. In this study, we focused on a detailed analysis of the SLP-76 N-terminal acidic region and its three tyrosine residues. These three tyrosine sites Y113, Y128 and Y145 are critical for TCR signalling and thymocyte development (Jordan *et al*, 2006, 2008). Earlier studies have shown that Nck and VAV1, which are known to bind SLP-76 at phosphorylated Y113 and Y128, have a critical function in the activation and actin polymerization pathways of T lymphocytes (Zeng *et al*, 2003). Nck recruits NPFs such as WASp to the IS where they activate the Arp2/3 complex and actin polymerization (Buday *et al*, 2002), whereas VAV1 acts as a GEF of Rho-family GTPase proteins that activate NPFs after stimulation (Tybulewicz, 2005). The existing model has been that cooperation between these proteins is essential and necessary for a complete T-cell immune response. This model is mainly based on biochemical studies, suggesting that SLP-76 functions as a necessary

scaffold that can bind both Nck and VAV1 (Bubeck Wardenburg *et al*, 1998; Zeng *et al*, 2003).

This model was generated primarily using coimmunoprecipitation, which is powerful, but limited. In our current work, we used ITC techniques to measure the affinity, stoichiometry and specificity of Nck and VAV1 binding to sites of tyrosine phosphorylation on SLP-76. AUC was used to further explore the stoichiometry of the complex and to address the potential cooperativity of protein binding. These experiments were performed using purified full-length Nck and a large polypeptide fragment of VAV1 containing its interaction domains to test binding to SLP-76 phosphopeptides. Finally, molecular imaging techniques were used to demonstrate intramolecular interactions *in vivo*. This analysis including FRET was supported by gene silencing and confirmatory biochemical experiments.

ITC analyses of VAV1 and Nck binding to short phosphopeptides (17-mers) with sequences centred at the three SLP-76 phosphotyrosines showed that VAV1 and Nck both bind at pY113 and pY128. There is no binding of VAV1 to pY145; Nck binds this site with low affinity. Unfortunately, our inability to purify Itk precluded studies of its binding to the pY145 site where it is thought to bind.

Additional results emerged during the study of longer peptides (49-mers) made with the SLP-76 sequence and containing two or three phosphorylated tyrosines. The thermodynamic analysis performed with the SEDPHAT software (Houtman *et al*, 2007) revealed that only one molecule of either VAV1 or Nck bound to phosphopeptides containing two phosphoproteins, either pY113 or pY128 with pY145. Surprisingly, only one molecule of VAV1 bound the doubly phosphorylated long peptide containing the two sites, pY113 and pY128, which are each alone capable of binding VAV1. Also of note was that two molecules of either VAV1 or Nck bound the triply phosphorylated long peptides. We cannot conclude that both pY113 and pY128 are occupied in these peptides, though that is what we would expect. However, we can conclude that phosphorylation at Y145 influences the binding, and it at least for the case of Nck binding, phosphorylation on this site is required for the 2:1 (Nck:SLP-76) stoichiometry.

AUC confirmed our ITC results and enabled us to probe higher-order complex formation. VAV1 and Nck individually mixed with doubly phosphorylated SLP-76 showed sedimentation profiles, suggesting a stoichiometry of binding of 1:1. VAV1 or Nck binding to the triply phosphorylated peptides generated an additional peak with a greater *s*-value consistent in both cases with the binding of two molecules to this peptide. These data are consistent with the results of the ITC analysis.

The strength of the multi-signal sedimentation velocity method is the capacity to track the inclusion of several molecular species in multi-molecular complexes. Thus, a mixture of VAV1 and Nck added to the doubly phosphorylated SLPpY113, 145 phosphopeptide resulted in a marked shift in sedimentation profile consistent with both Nck and VAV1 binding to the SLP-76 phosphopeptide with a 1:1:1 stoichiometry. The mechanism of binding, that is, whether both proteins bind to the two sites or whether a complex of the two binds to one site cannot be determined. The AUC sedimentation of the mix of VAV1 and Nck with the triply phosphorylated peptide was even more striking. In this case, the sedimentation pattern suggests three or even four molecules bound to the phosphopeptide. In the latter case, the binding stoichiometry of VAV1 to Nck to peptide was likely 2:2:1. From this result, one would have to conclude that Nck and VAV1 interacted directly in the complex even though we only observed a weak interaction of these proteins in the absence of SLP-76 with purified preparations. Moreover, one and perhaps two Nck–VAV1 complexes would bind SLP-76, one at pY113 and one at pY128, with pY145 again in some way enabling these binding events.

We turned to molecular imaging and specifically to FRET analysis to further study the binding properties of these proteins in intact, living cells. Nck binding to SLP-76 was shown to be independent of VAV1 as the level of FRET efficiency between Nck and SLP-76 was unaffected in VAV1-deficient cells. It is important to emphasis the point that our data did not support an interaction between Nck to VAV2 and/or VAV3, eliminating the involvement of these proteins in the recruitment of Nck to SLP-76 in the absence of VAV1.

In our *in vitro* studies, VAV1 binding to SLP-76 was readily detected. Surprisingly, *in vivo* binding of VAV1 to SLP-76 was very weak in the absence of Nck. We note that for technical reasons, we used a large polypeptide fragment of VAV1 for our binding studies and not the full-length protein. This difference and the possibility of multiple, cooperative-binding events *in vivo* in the setting of numerous other binding events may account for this difference in the *in vitro* and *in vivo* results.

As VAV1 interaction with SLP-76 *in vivo* is dependent on Nck binding, we tested the function of the individual Nck-binding sites on SLP-76 for VAV1 binding. FRET efficiency between SLP-76 and VAV1 molecules tagged with fluorescent proteins was detected in VAV1-deficient T cells (J-VAV cells). The interaction between these proteins decreased when either the SLP-76Y113F or SLP-76Y128F mutant was used. When we mutated both sites (Y113 and Y128), the FRET efficiency between SLP-76 and VAV1 was dramatically reduced. Thus, each of the two SLP-76 phosphotyrosine residues that bind Nck contributes to VAV1 recruitment. FRET was not completely abolished with the mutation of Y113 and Y128, so a weak interaction of Nck at phosphorylated Y145 is possible.

Further analysis revealed that the Nck requirement for VAV1 binding reflected the fact that Nck interacts directly with VAV1. This association depends on binding between the C-terminal SH3 domain of Nck and proline residues in the N-terminal VAV1 SH3 domain. Our conclusion from the imaging studies of the Nck–VAV1 interaction shed light on the AUC results. We suggest that it is likely that two Nck–VAV1 dimers bind phosphorylated SLP-76 through the interaction of the Nck SH2 domain with SLP-76 (Figure 7A). However, based on the ITC data, we do not rule out the possibility that minor fraction of VAV1 directly associate to SLP-76 after TCR stimulation as suggested by Wu *et al* (1996) (Figure 7B). The question of whether multiple SLP-76 molecules interact in a complex has been raised earlier (Jordan *et al*, 2008). Our AUC data do not support this idea, but our cellular data do not address this point. Regardless of the exact orientation of molecules, it is clear that the binding of Nck, VAV1 and SLP-76 is highly cooperative within the cell.

Our mapping of the Nck–VAV1 interaction was simplified by a sequence alignment between the SH3 C-terminal

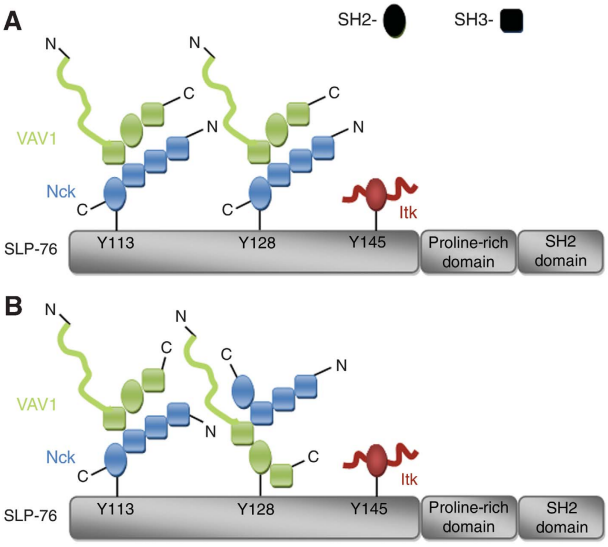

Figure 7 Schematic representation of possible oligomerization models of SLP-76-binding sites (**A**, **B**). On TCR activation, SLP-76 is fully phosphorylated. This event leads to the oligomerization of SLP-76 by Nck and VAV1 and possibly Itk-containing complexes. The oligomerized SLP-76 molecules then serve as a nucleation site for other signalling molecules, resulting in the activation of intracellular signalling pathways.

domains of Nck and Grb-2, which showed a high homology between the two. As Grb-2 is a known VAV1-binding protein (Ye and Baltimore, 1994), it is possible that Nck competes with Grb-2 for the binding to VAV1. We have found that the interaction between Nck and VAV1 is constitutive and is upregulated by TCR activation. These results were confirmed in primary T cells.

Functional studies have shown that the point mutation in the VAV1 N-terminal SH3 domain, which alters the direct interaction between Nck and VAV1, has minimal effects on ZAP-70, LAT or PLCγ1 phosphorylation or Ca^{2+} flux, but causes severe defects in actin reorganization. To date, most if not all studies relating to the regulation of actin machinery have indicated the central function of SLP-76 in actin rearrangement (Zeng *et al*, 2003; Barda-Saad *et al*, 2005). One of the questions frequently raised was how SLP-76-deficient T cells organize their actin cytoskeleton. Our finding that Nck and VAV1 directly interact independently of SLP-76 partially addresses this question. Experiments with Jurkat T cells expressing a tyrosine mutant of SLP-76 (Y3F) showed that VAV1 recruitment to the IS was diminished but not completely abrogated (Zeng *et al*, 2003). In addition, an SLP-76 mutant that contains tyrosine to phenylalanine substitutions at positions 112, 128 and thus lacking the VAV1-binding sites exhibited a reduction in VAV1 association but not a complete blockage (Jordan *et al*, 2006, 2008), indicating an alternative indirect binding site possibly through Y145 that binds Nck. An additional possible mechanism for actin polymerization in the absence of SLP-76 is the function of alternative NPFs other than WASp, such as WAVE2, HS1 and others (Gomez *et al*, 2006, 2007; Nolz *et al*, 2006; Zipfel *et al*, 2006; Schwartzberg, 2007). Recently, WAVE2 has been shown to have a central function in actin polymerization (Nolz *et al*, 2006; Zipfel *et al*, 2006). Although WASp and WAVE2 share several structural features and are involved in the formation of actin-rich structures (Billadeau and Burkhardt, 2006; Nolz *et al*, 2006; Zipfel *et al*, 2006; Takenawa and Suetsugu, 2007) they are involved in different actin-mediated events. Whereas WASp has been implicated in vesicular trafficking and endocytosis (McGavin *et al*, 2001; Schafer, 2002), WAVE2 was shown to control integrin-mediated adhesion (Billadeau *et al*, 2007). However, whereas the molecular cascade linking WASp to TCR site was defined, the molecular mechanism that couples WAVE2 to the IS remains mostly unknown (Billadeau and Burkhardt, 2006). Thus, further studies are required to better identify and define the function of the NPFs regulated by Nck:VAV1 molecular complexes suggested by this work.

Materials and methods

Reagents

Mouse anti-CD3 and anti-CD28 were purchased from BD Biosciences. Primary antibodies were purchased from the following suppliers: anti-GFP was purchased from Roche, this antibody cross-reacts with YFP and CFP; anti-Nck from Upstate; anti-VAV1 used for immunoprecipitation from Epitomics; anti-VAV1 and anti-panVAV for immunoblotting from Santa Cruz; anti-VAV3 was kindly provided by Daniel D Billadeau (University of Minnesota, Minneapolis, MN), anti-phosphoTyrosine 4G10 from Upstate; phalloidin from Molecular Probes. Nckα&β targeted siRNA or irrelevant siRNA (SMARTpool) were purchased from Dharmacon. VAV2 and VAV3 targeted siRNA from Santa Cruz.

Plasmid construction and GFP mutation

Human Nck wt and individually SH3-point mutated Nck cDNA were kindly provided by B Mayer (University of Connecticut Health Center, Farmington, CT). The cDNA was cloned into the expression vector pECFP-C or pEYFP-C to obtain the CFP- or YFP-tagged Nck. GFP derivates used were rendered monomeric by a published A206K substitution (Zacharias *et al*, 2002).

Cell transfection and generation of stable cells

Cells were transfected with an AMAXA electroporator using AMAXA solution T and protocol H-10. Stable clones were derived from transiently transfected cells with a combination of drug selection and cell sorting. Cells transiently expressing chimeras were selected in either neomycin (parental Clontech vectors) or hygromycin (vectors with a pcDNA3.1$^+$Hygro backbone). Cell fluorescence analysis and cell sorting were done on a FACSVantage (Becton Dickinson Biosciences).

PBL isolation and stimulation

Human PBLs were isolated from whole blood of healthy donors as described earlier (Barda-Saad *et al*, 2005). The cells were then stimulated with anti-CD3 (OKT3 ascites, 1/200) and anti-CD28 (10 μg/ml) for 30 min on ice. Cells were warmed at 37°C for 10 min and stimulated with anti-mouse IgG (50 μg/ml) for 2 min.

Spreading assay and molecular imaging

The spreading assays were performed as described earlier (Bunnell *et al*, 2002; Barda-Saad *et al*, 2005) Dynamic fluorescent and interference reflection microscopy images were collected on a Zeiss LSM510 Meta confocal microscope. All images were collected with a ×63 Plan-Apochromat objective (Carl Zeiss).

FRET analysis

FRET was measured by the donor-sensitized acceptor fluorescence technique as described earlier (Barda-Saad *et al*, 2005). Briefly, three sets of filters were used: one optimized for donor fluorescence (excitation, 468 nm; emission, 475–505 nm); a second, for acceptor fluorescence (excitation, 514 nm; emission, 530 nm LP) and a third, for FRET (excitation, 468 nm; emission, 530 nm LP). FRET was corrected and its efficiency was determined as described in detail in Supplementary data. To estimate the importance of the obtained FRET efficiency values and to exclude the possibility of obtaining false-positive FRET, we prepared cells expressing free CFP and free YFP as negative controls. The FRET efficiency in the negative

control system was measured and calculated in the same way as in the main experiment. FRET efficiency values obtained from the negative control samples were subtracted from the values obtained in the main experiments.

Immunoblotting and immunoprecipitation

Jurkat cells were either stimulated with anti-CD3 C305 for 2 min or left untreated. The optimal concentration of the stimulatory antibody was determined by titration. Protein A/G Plus-Agarose beads (Santa Cruz Biotechnology) were used for immunoprecipitation. Protein samples were resolved on sodium dodecyl sulfate–polyacrylamide gel electrophoresis (SDS–PAGE), transferred to nitrocellulose membrane, and immunoblotted with appropriate primary antibodies. Immunoreactive proteins were detected with either anti-mouse or anti-rabbit horseradish peroxidase-coupled secondary antibody followed by detection with enhanced chemiluminescence (Pierce). The lanes 'No Ab' define the negative control samples. The samples represent cell lysates, which underwent the same procedure as the experimental samples in the absence of a specific antibody to eliminate the possibility of non-specific binding between the cell lysates and the beads.

Luciferase assay

Cells were transiently cotransfected with 15 μg of an NFAT luciferase reporter plasmid along with the plasmids indicated in the figure legends. After 16–20 h, cells were aliquoted into a 96-well cell culture dish at 2×10^5 cells/well and stimulated for 6 h at 37°C, with the stimuli indicated in the figure legends. Cells were lysed and assayed for luciferase activity as described earlier (Gonen *et al*, 2005). To correct for variations in transfection efficiency, the NFAT luciferase activity obtained on receptor stimulation was normalized to the activity obtained on treatment with phorbol 12-myristate 13-acetate (50 ng/ml) plus ionomycin (1 μM).

Analytical ultracentrifugation

The SH3–SH2–SH3 domains of VAV1, corresponding to residues 580–845 and full-length human Nck were expressed and purified. SLP-76 peptides were synthesized (see Supplementary data).

Centrifugation experiments were carried out in a ProteomeLab XL-I analytical ultracentrifuge (Beckman Coulter, Palo Alto, CA) as described earlier (Brown *et al*, 2008). SLP-76 peptides were end labelled with rhodamine TAMRA, as above, allowing for their specific detection in the absorbance optical system at 555 nm. VAV1 was modified with a site-specific label (VAV1-FAM), as described in detail in Supplementary data, for detection at 494 nm. In a control experiment, VAV1-FAM was shown by ITC to have unaltered binding properties to SLP-76 peptides. Sv experiments were conducted with 400 μl samples of both proteins at equimolar (4 or 6 μM) concentration, at a four-molar excess relative to the SLP-76 peptide (at 1 or 1.5 μM), dissolved in PBS. Sedimentation took place in an 8-hole rotor at 50 000 r.p.m. at a temperature of 20°C, and absorbance profiles at 494 and 555 nm and interference optical profiles were acquired in intervals of 15 min. The data were analysed in SEDPHAT with the $c_k(s)$ method (Balbo *et al*, 2005). The molar sedimentation coefficient distributions for the SLP-76 peptide were integrated to determine the concentration and average sedimentation coefficient of the protein/peptide complexes.

Statistical analyses

All graphs were prepared with the use of Microsoft Excel. Standard errors were calculated with the use of Microsoft Excel. Statistical significances were calculated in Kaleidagraph or Excel, with Student's *t*-tests used for unpaired samples. In all cases, the threshold *P*-value required for significance was 0.05.

Supplementary data

Supplementary data are available at *The EMBO Journal* Online (http://www.embojournal.org).

Acknowledgements

We thank Dr Alex Braiman for his help with the calcium measurement analysis and Uriel Kaaro for his help in the operation of the FACS sorting. This work was supported, in part, by the Intramural Research Program of NCI and NIBIB, NIH and in part by the Israel Science Foundation (grants no. 971/08 and 1659/08).

Conflict of interest

The authors declare that they have no conflict of interest.

References

Astoul E, Laurence AD, Totty N, Beer S, Alexander DR, Cantrell DA (2003) Approaches to define antigen receptor-induced serine kinase signal transduction pathways. *J Biol Chem* **278:** 9267–9275

Badour K, Zhang J, Shi F, McGavin MK, Rampersad V, Hardy LA, Field D, Siminovitch KA (2003) The Wiskott-Aldrich syndrome protein acts downstream of CD2 and the CD2AP and PSTPIP1 adaptors to promote formation of the immunological synapse. *Immunity* **18:** 141–154

Balbo A, Minor KH, Velikovsky CA, Mariuzza RA, Peterson CB, Schuck P (2005) Studying multiprotein complexes by multisignal sedimentation velocity analytical ultracentrifugation. *Proc Natl Acad Sci USA* **102:** 81–86

Barda-Saad M, Braiman A, Titerence R, Bunnell SC, Barr VA, Samelson LE (2005) Dynamic molecular interactions linking the T cell antigen receptor to the actin cytoskeleton. *Nat Immunol* **6:** 80–89

Billadeau DD, Burkhardt JK (2006) Regulation of cytoskeletal dynamics at the immune synapse: new stars join the actin troupe. *Traffic* **7:** 1451–1460

Billadeau DD, Nolz JC, Gomez TS (2007) Regulation of T-cell activation by the cytoskeleton. *Nat Rev Immunol* **7:** 131–143

Braiman A, Barda-Saad M, Sommers CL, Samelson LE (2006) Recruitment and activation of PLCgamma1 in T cells: a new insight into old domains. *EMBO J* **25:** 774–784

Brown PH, Balbo A, Schuck P (2008) Characterizing protein-protein interactions by sedimentation velocity analytical ultracentrifugation. *Curr Protoc Immunol* Chapter 18: Unit 18.15

Bubeck Wardenburg J, Pappu R, Bu JY, Mayer B, Chernoff J, Straus D, Chan AC (1998) Regulation of PAK activation and the T cell cytoskeleton by the linker protein SLP-76. *Immunity* **9:** 607–616

Buday L, Wunderlich L, Tamas P (2002) The Nck family of adapter proteins: regulators of actin cytoskeleton. *Cell Signal* **14:** 723–731

Bunnell SC, Diehn M, Yaffe MB, Findell PR, Cantley LC, Berg LJ (2000) Biochemical interactions integrating Itk with the T cell receptor-initiated signaling cascade. *J Biol Chem* **275:** 2219–2230

Bunnell SC, Hong DI, Kardon JR, Yamazaki T, McGlade CJ, Barr VA, Samelson LE (2002) T cell receptor ligation induces the formation of dynamically regulated signaling assemblies. *J Cell Biol* **158:** 1263–1275

Bunnell SC, Kapoor V, Trible RP, Zhang W, Samelson LE (2001) Dynamic actin polymerization drives T cell receptor-induced spreading: a role for the signal transduction adaptor LAT. *Immunity* **14:** 315–329

Burkhardt JK, Carrizosa E, Shaffer MH (2008) The actin cytoskeleton in T cell activation. *Annu Rev Immunol* **26:** 233–259

Cannon JL, Labno CM, Bosco G, Seth A, McGavin MH, Siminovitch KA, Rosen MK, Burkhardt JK (2001) Wasp recruitment to the T cell: APC contact site occurs independently of Cdc42 activation. *Immunity* **15:** 249–259

Cao Y, Janssen EM, Duncan AW, Altman A, Billadeau DD, Abraham RT (2002) Pleiotropic defects in TCR signaling in a Vav-1-null Jurkat T-cell line. *EMBO J* **21:** 4809–4819

Clements JL (2003) Known and potential functions for the SLP-76 adapter protein in regulating T-cell activation and development. *Immunol Rev* **191:** 211–219

Dombroski D, Houghtling RA, Labno CM, Precht P, Takesono A, Caplen NJ, Billadeau DD, Wange RL, Burkhardt JK, Schwartzberg PL (2005) Kinase-independent functions for Itk in TCR-induced

regulation of Vav and the actin cytoskeleton. *J Immunol* **174:** 1385–1392

Dustin ML (2008) T-cell activation through immunological synapses and kinapses. *Immunol Rev* **221:** 77–89

Fang N, Motto DG, Ross SE, Koretzky GA (1996) Tyrosines 113, 128, and 145 of SLP-76 are required for optimal augmentation of NFAT promoter activity. *J Immunol* **157:** 3769–3773

Fuller CL, Braciale VL, Samelson LE (2003) All roads lead to actin: the intimate relationship between TCR signaling and the cytoskeleton. *Immunol Rev* **191:** 220–236

Gomez TS, Kumar K, Medeiros RB, Shimizu Y, Leibson PJ, Billadeau DD (2007) Formins regulate the actin-related protein 2/3 complex-independent polarization of the centrosome to the immunological synapse. *Immunity* **26:** 177–190

Gomez TS, McCarney SD, Carrizosa E, Labno CM, Comiskey EO, Nolz JC, Zhu P, Freedman BD, Clark MR, Rawlings DJ, Billadeau DD, Burkhardt JK (2006) HS1 functions as an essential actin-regulatory adaptor protein at the immune synapse. *Immunity* **24:** 741–752

Gonen R, Beach D, Ainey C, Yablonski D (2005) T cell receptor-induced activation of phospholipase C-gamma1 depends on a sequence-independent function of the P-I region of SLP-76. *J Biol Chem* **280:** 8364–8370

Houtman JC, Brown PH, Bowden B, Yamaguchi H, Appella E, Samelson LE, Schuck P (2007) Studying multisite binary and ternary protein interactions by global analysis of isothermal titration calorimetry data in SEDPHAT: application to adaptor protein complexes in cell signaling. *Protein Sci* **16:** 30–42

Houtman JC, Higashimoto Y, Dimasi N, Cho S, Yamaguchi H, Bowden B, Regan C, Malchiodi EL, Mariuzza R, Schuck P, Appella E, Samelson LE (2004) Binding specificity of multiprotein signaling complexes is determined by both cooperative interactions and affinity preferences. *Biochemistry* **43:** 4170–4178

Houtman JC, Yamaguchi H, Barda-Saad M, Braiman A, Bowden B, Appella E, Schuck P, Samelson LE (2006) Oligomerization of signaling complexes by the multipoint binding of GRB2 to both LAT and SOS1. *Nat Struct Mol Biol* **13:** 798–805

Jordan MS, Sadler J, Austin JE, Finkelstein LD, Singer AL, Schwartzberg PL, Koretzky GA (2006) Functional hierarchy of the N-terminal tyrosines of SLP-76. *J Immunol* **176:** 2430–2438

Jordan MS, Smith JE, Burns JC, Austin JE, Nichols KE, Aschenbrenner AC, Koretzky GA (2008) Complementation in trans of altered thymocyte development in mice expressing mutant forms of the adaptor molecule SLP76. *Immunity* **28:** 359–369

Kane LP, Lin J, Weiss A (2000) Signal transduction by the TCR for antigen. *Curr Opin Immunol* **12:** 242–249

Kliche S, Breitling D, Togni M, Pusch R, Heuer K, Wang X, Freund C, Kasirer-Friede A, Menasche G, Koretzky GA, Schraven B (2006) The ADAP/SKAP55 signaling module regulates T-cell receptor-mediated integrin activation through plasma membrane targeting of Rap1. *Mol Cell Biol* **26:** 7130–7144

Koretzky GA, Abtahian F, Silverman MA (2006) SLP76 and SLP65: complex regulation of signalling in lymphocytes and beyond. *Nat Rev Immunol* **6:** 67–78

Ladbury JE (2007) Measurement of the formation of complexes in tyrosine kinase-mediated signal transduction. *Acta Crystallogr D Biol Crystallogr* **63:** 26–31

Laurence A, Astoul E, Hanrahan S, Totty N, Cantrell D (2004) Identification of pro-interleukin 16 as a novel target of MAP kinases in activated T lymphocytes. *Eur J Immunol* **34:** 587–597

McGavin MK, Badour K, Hardy LA, Kubiseski TJ, Zhang J, Siminovitch KA (2001) The intersectin 2 adaptor links Wiskott Aldrich Syndrome protein (WASp)-mediated actin polymerization to T cell antigen receptor endocytosis. *J Exp Med* **194:** 1777–1787

Nishida M, Nagata K, Hachimori Y, Horiuchi M, Ogura K, Mandiyan V, Schlessinger J, Inagaki F (2001) Novel recognition mode between Vav and Grb2 SH3 domains. *EMBO J* **20:** 2995–3007

Nolz JC, Gomez TS, Zhu P, Li S, Medeiros RB, Shimizu Y, Burkhardt JK, Freedman BD, Billadeau DD (2006) The WAVE2 complex regulates actin cytoskeletal reorganization and CRAC-mediated calcium entry during T cell activation. *Curr Biol* **16:** 24–34

Raab M, da Silva AJ, Findell PR, Rudd CE (1997) Regulation of Vav-SLP-76 binding by ZAP-70 and its relevance to TCR zeta/CD3 induction of interleukin-2. *Immunity* **6:** 155–164

Reynolds LF, Smyth LA, Norton T, Freshney N, Downward J, Kioussis D, Tybulewicz VL (2002) Vav1 transduces T cell receptor signals to the activation of phospholipase C-gamma1 via phosphoinositide 3-kinase-dependent and -independent pathways. *J Exp Med* **195:** 1103–1114

Schafer DA (2002) Coupling actin dynamics and membrane dynamics during endocytosis. *Curr Opin Cell Biol* **14:** 76–81

Schwartzberg PL (2007) Formin the way. *Immunity* **26:** 139–141

Smith-Garvin JE, Koretzky GA, Jordan MS (2009) T cell activation. *Annu Rev Immunol* **27:** 591–619

Sohn HW, Tolar P, Jin T, Pierce SK (2006) Fluorescence resonance energy transfer in living cells reveals dynamic membrane changes in the initiation of B cell signaling. *Proc Natl Acad Sci USA* **103:** 8143–8148

Takenawa T, Suetsugu S (2007) The WASP-WAVE protein network: connecting the membrane to the cytoskeleton. *Nat Rev Mol Cell Biol* **8:** 37–48

Tybulewicz VL (2005) Vav-family proteins in T-cell signalling. *Curr Opin Immunol* **17:** 267–274

Wallrabe H, Periasamy A (2005) Imaging protein molecules using FRET and FLIM microscopy. *Curr Opin Biotechnol* **16:** 19–27

Wu J, Motto DG, Koretzky GA, Weiss A (1996) Vav and SLP-76 interact and functionally cooperate in IL-2 gene activation. *Immunity* **4:** 593–602

Wu JN, Koretzky GA (2004) The SLP-76 family of adapter proteins. *Semin Immunol* **16:** 379–393

Wunderlich L, Farago A, Downward J, Buday L (1999) Association of Nck with tyrosine-phosphorylated SLP-76 in activated T lymphocytes. *Eur J Immunol* **29:** 1068–1075

Yablonski D, Kuhne MR, Kadlecek T, Weiss A (1998) Uncoupling of nonreceptor tyrosine kinases from PLC-gamma1 in an SLP-76-deficient T cell. *Science* **281:** 413–416

Ye ZS, Baltimore D (1994) Binding of Vav to Grb2 through dimerization of Src homology 3 domains. *Proc Natl Acad Sci USA* **91:** 12629–12633

Zacharias DA, Violin JD, Newton AC, Tsien RY (2002) Partitioning of lipid-modified monomeric GFPs into membrane microdomains of live cells. *Science* **296:** 913–916

Zeng R, Cannon JL, Abraham RT, Way M, Billadeau DD, Bubeck-Wardenberg J, Burkhardt JK (2003) SLP-76 coordinates Nck-dependent Wiskott-Aldrich syndrome protein recruitment with Vav-1/Cdc42-dependent Wiskott-Aldrich syndrome protein activation at the T cell-APC contact site. *J Immunol* **171:** 1360–1368

Zhang W, Sloan-Lancaster J, Kitchen J, Trible RP, Samelson LE (1998) LAT: the ZAP-70 tyrosine kinase substrate that links T cell receptor to cellular activation. *Cell* **92:** 83–92

Zipfel PA, Bunnell SC, Witherow DS, Gu JJ, Chislock EM, Ring C, Pendergast AM (2006) Role for the Abi/wave protein complex in T cell receptor-mediated proliferation and cytoskeletal remodeling. *Curr Biol* **16:** 35–46

